Influence of rotation-induced nuclear deformation on α-particle evaporation spectra

J. R. Huizenga, A. N. Behkami, I. M. Govil, W. U. Schröder, and J. Tõke
Department of Chemistry and Nuclear Structure Research Laboratory, University of Rochester, Rochester, New York 14627
(Received 22 March 1989)

The shapes of α-particle spectra from hot, high-spin compound nuclei produced in energetic heavy-ion fusion reactions are analyzed within the framework of a statistical model. Contrary to claims made in the literature, good agreement is obtained between calculated and experimental spectra when the evaporation barrier of each nuclide in the complex cascade is assumed equal to its respective absorption channel barrier. The dependence of the shape of α-particle spectra on nuclear deformation is discussed both in terms of the transmission coefficients and the spin-dependent level density of deformed nuclei. For deformations of the magnitude given by the rotating liquid drop model, α-particle spectra and effective barriers are insensitive to whether deformed or spherical nucleus transmission coefficients are used. It is important, however, to include the deformation dependence in the nuclear level density. Model calculations indicate that the shape of α-particle spectra may be quite insensitive to large deformations.

I. INTRODUCTION

Considerable effort has been made in the past to understand the spectra of charged particles evaporated from excited nuclear systems prepared in various ways. The motivations for these studies has been twofold.[1] On the one hand, such spectral data, along with their analyses, provide a method to study the properties of equilibrated nuclear systems as a function of excitation energy, angular momentum, and deformation. On the other hand, a profound understanding of particle evaporation spectra and multiplicities is a prerequisite for employing charged-particle emission as a potentially powerful probe of equilibration processes in nuclear collisions, and of various additional aspects of the collision dynamics.

Standard statistical models[2–10] have been employed for many years to study the decay of composite nuclei at moderate energies and angular momenta, such as those produced with light-ion projectiles.[11–18] Several of these studies have shown that spectra can be reproduced using particle transmission coefficients calculated from optical models for the inverse reaction. Even for light-ion-induced reactions, however, it is usually necessary to use an angular-momentum-dependent theory in fitting angular and energy-dependent differential cross sections.

Over the last decade, however, many papers have claimed[19–30] that experimental charged-particle evaporation spectra from heavy-ion fusion reactions, where higher excitation energies and angular momenta are involved, are no longer consistent with predictions of standard statistical models. Specifically, it has been suggested that for heavy-ion-induced reactions the charged-particle emission barriers are significantly lower than those calculated with optical-model transmission coefficients for the respective inverse absorption channels. In fact, several authors claim that spectra data require composite nuclei with unusually large deformations[22,25,27,28] (e.g., with axis ratios ranging from 2.2 to 3.0), much in excess of predictions based on the rotating liquid drop model.[31]

In order to evaluate the reported claims of very deformed nuclear shapes based on charged-particle spectra, a program was initiated to compare available experimental α-particle spectra from heavy-ion-induced reactions with theoretical results from a standard statistical model. This model incorporates a spin-dependent level density that accounts, in an approximate way, for the spin-dependent shape changes predicted by the rotating liquid drop model (RLDM). First results[1] showed good agreement between calculated and experimental α-particle spectra for the ^{27}Al+^{40}Ar reaction without the need to lower the evaporation barriers relative to the respective absorption barriers, suggesting the analyses of other experimental α-particle spectra from heavy-ion-induced fusion reactions. The results of these analyses, confirming previous conclusions, are reported here. In addition, a number of model calculations are performed to study the effect of nuclear deformation on α-particle spectra. In Sec. II, a procedure for the calculation of evaporation spectra is described. The results of model calculations of spectra from deformed nuclei are presented in Sec. III. Theoretical statistical model fits to experimental α-particle spectra are presented and discussed in Sec. IV. A summary is included in Sec. V.

II. CALCULATION OF EVAPORATION SPECTRA

In the present work, a slightly modified version of the statistical-model computer code CASCADE (Ref. 32) has been employed in the analysis of particle evaporation spectra. This version calculates proper energy spectra in the c.m. system, rather than the total kinetic energy (including recoil) distributions predicted by the original code, which cannot be compared directly to experimental data. In the statistical model,[2–10] there are two basic quantities that govern the flow of an evaporation cascade. These are the spin-dependent level density, defining the available phase space and the transmission coefficients

that control access to this space. The change in each of these quantities with deformation is considered here.

For calculating the spin-dependent level density, the code CASCADE assumes the analytical expression

$$\rho(E,I)=\frac{a^{1/2}}{24\sqrt{2}}\frac{\hbar^3}{J_0^{3/2}}\frac{(2I+1)}{(E+t-\Delta-E_I)^2}\times\exp\{2[a(E-\Delta-E_I)]^{1/2}\}\ , \quad (1)$$

where a is the level-density parameter, and t is the thermodynamic temperature. This level-density formula is based on an approximation of a Fermi gas with equidistant single-particle levels and a constant level-density parameter (assumed to be $a=A/8$). While such a simple nuclear model clearly has insufficiencies, it is assumed that it can be used to approximate the level density at the total excitation energy E and spin I by evaluating the model level density at an energy reduced by a pairing correction Δ and a *spin-dependent parameter* E_I. In the calculation, the quantity E_I is parametrized as

$$E_I=(\hbar^2/2J_0)I(I+1)/(1+\delta_1 I^2+\delta_2 I^4)\ , \quad (2)$$

in terms of the rigid-body moment of inertia J_0 of a spherical nucleus (the radius parameter r_0 in CASCADE depends slightly on A, e.g., 1.26 and 1.28 fm for the compound nuclei ^{67}Ga and ^{59}Cu, respectively). The quantities δ_1 and δ_2 are adjustable input parameters providing a range of choices for the spin dependence of the level density.

In the application of the above formula to nuclei of high spins and excitation energies, it must be emphasized that E_I is not necessarily the yrast energy. In particular, this quantity should be equated neither to the yrast energy of a rigid body with a spin-independent moment of inertia as employed by Lang[33] nor to the yrast energy (collective rotational plus deformation energy) of a rigid body with a spin-dependent moment of inertia. In general, the quantity E_I has a much more complex interpretation. This is due, in part, to the rearrangement of the single-particle levels near the Fermi energy that is associated with the spin-dependent nuclear deformation, and the direct effect of this nuclear structure change on the spin-dependent level density. In the present formulation of $\rho(E,I)$ any dependence of the level-density parameter a on spin or deformation is incorporated into E_I. The dependence of the level density on deformation caused by periodic changes in the shell structure is well known for the low-spin systems.[17,34] In the high-energy limit, the shell effect on the level density can be described in terms of a constant correction to the intrinsic excitation energy at which this density is to be derived using a Fermi gas formula. It will be shown later that the dependence of the level density on excitation energy and spin is a crucial quantity in statistical-model calculations for heavy-ion-induced reactions. However, very little is known experimentally about this spin dependence for the large spins and high excitation energies of interest here. Therefore, to achieve the best fit to experimental data, it appears justifiable to select to some extent a spin dependence of the level density, e.g., by adjusting the parameters δ_1 and δ_2 in Eq. (2).

While the above discussion referred to the phase space, in the following the transmission coefficients describing the access to this phase space are considered. In the standard application of CASCADE, the transmission coefficients are those for spherical nuclei, including neutron,[35] proton,[36] and α-particle[37] emission, and are generated with published optical-model parameters. As in all such calculations, the present calculations of transmission coefficients for a particular decay process are based on the standard assumption that the respective inverse reaction (i.e., fusion on excited target nuclei) cross sections are well approximated by the total reaction cross sections for cold target nuclei. However, for the present study this concept has to be generalized to deformed nuclei, for which no data exists for inverse reactions.

Transmission coefficients for deformed nuclei were generated using a simple approximate procedure. In this procedure, the nucleus was represented by an ellipsoid of revolution (see Fig. 1) defined by

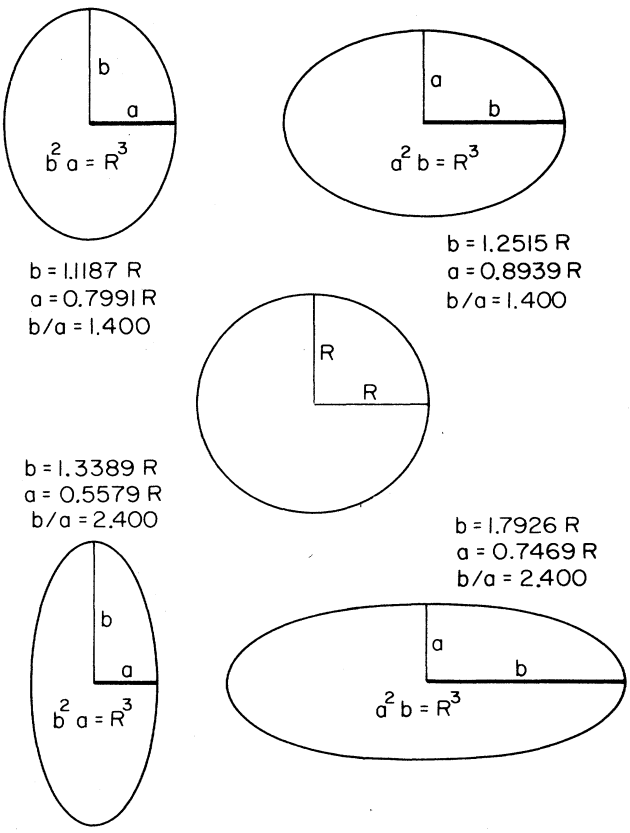

FIG. 1. Nuclear shapes utilized in calculations of α-particle transmission coefficients and spectra. Volume conservation is assumed in the calculation of the lengths of the axes for the symmetric prolate and oblate shapes with sharp surfaces. The heavy line in each prolate and oblate shape represents the symmetry axis (see Fig. 2).

$$\frac{x^2}{b^2}+\frac{y^2}{a^2}=1, \quad \frac{x^2}{a^2}\ \frac{y^2}{b^2}=1\ , \tag{3}$$

for prolate and oblate shapes, respectively. Here, the x axis is the symmetry axis, and y is perpendicular to x. The deformation is characterized by an axis ratio b/a, for a fixed volume equal to that of a sphere of radius R. Volume conservation then requires $a^2b=R^3$ for a prolate, and $ab^2=R^3$ for an oblate shape. The nucler radius varies with the angle Θ measured from the symmetry axis, i.e., $R=(x^2+y^2)^{1/2}$. The optical-model calculation for spherical nuclei was repeated for different radii, corresponding to a number of selected (x,y) pairs on the deformed nuclear surface. The transmission coefficients from these calculations were then weighted with the corresponding surface areas (see Fig. 2) to obtain effective transmission coefficients for deformed nuclei.

The resulting α-particle transmission coefficients for the ^{63}Cu$+\alpha$ reaction are shown in Figs. 3–5. At an energy equal to the barrier energy for emission of an α particle, the $l=0$ transmission coefficient assumes a value of $\frac{1}{2}$. In Fig. 3 the transmission coefficients for $l=0$ and 5 waves are plotted as a function of α-particle energy for prolate $(b/a=1.4)$, spherical, and oblate $(b/a=1.4)$ nuclear shapes. In each case, the three curves are essentially identical, with no appreciable difference in the effective barriers for the deformed and the spherical shapes. Similar results are illustrated in Fig. 4 for the more highly deformed prolate $(b/a=2.4)$ and oblate $(b/a=2.4)$ shapes. Again for the same reaction, the transmission coefficients for α particles with center-of-mass energies of 12.5 and 28.5 MeV are plotted as a function of angular momentum in Fig. 5 for spherical, prolate, and oblate nuclei, each of the latter two at deformations of $b/a=1.4$ and $b/a=2.4$.

As expected, deformed nuclei emit α particle with larger angular momenta than spherical nuclei. The present results shown in Fig. 5 are in qualitative agreement with earlier results,[38] calculated in a classical sharp-cutoff model with similar weighting over the surface area. As a consequence of these large angular momenta, α-particle spectra for deformed nuclei are harder. On the other hand, the reduction in transmission for smaller angular momenta for deformed nuclei is a direct consequence of the minor axis being smaller than R.

The error introduced in the present transmission

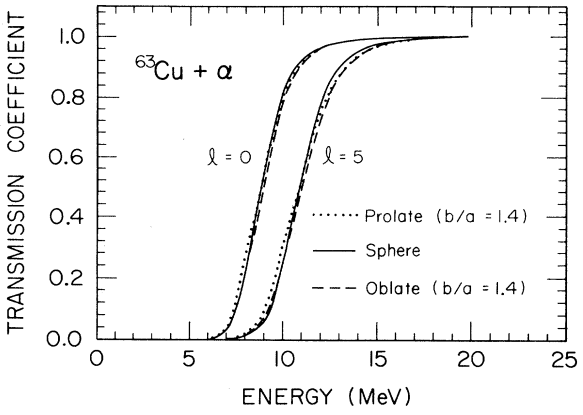

FIG. 3. α-particle transmission coefficients for the ^{63}Cu$+\alpha$ reaction, for $l=0$ and $l=5$ waves, are plotted as a function of α-particle energy for prolate $(b/a=1.4)$, spherical, and oblate $(b/a=1.4)$ nuclear shapes. The procedure for calculating the transmission coefficients for deformed nuclei is described in the text.

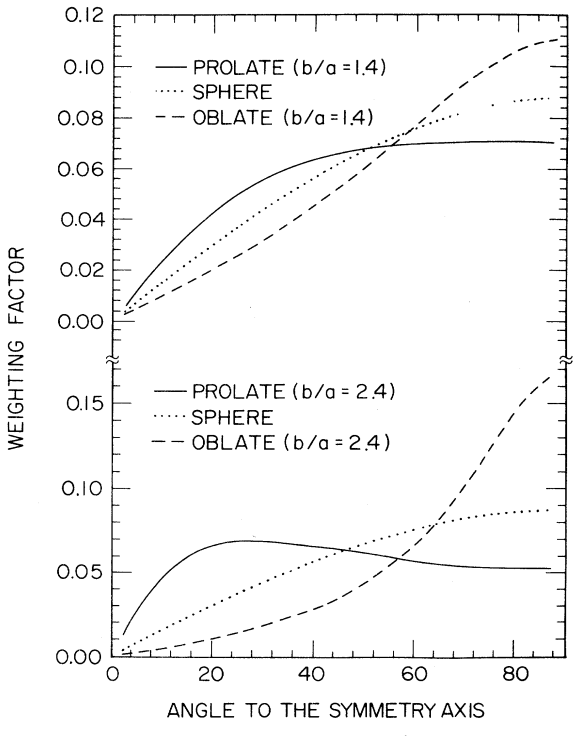

FIG. 2. Surface-weighted intensity factors for particle emission as a function of angle to the symmetry axis for prolate, oblate, and spherical shapes (see Fig. 1).

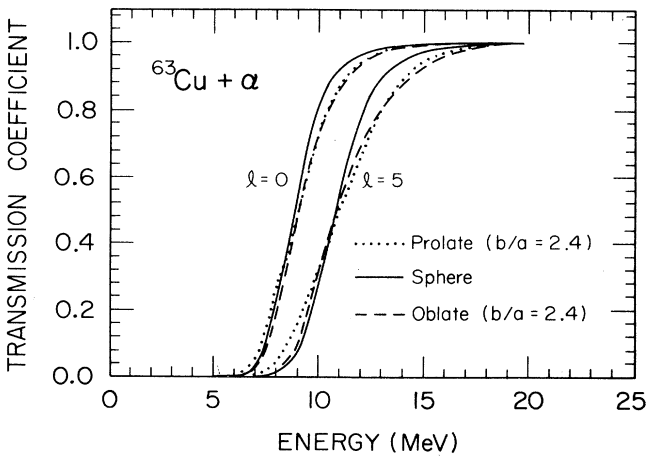

FIG. 4. Same as Fig. 3 except for a deformation of $b/a=2.4$.

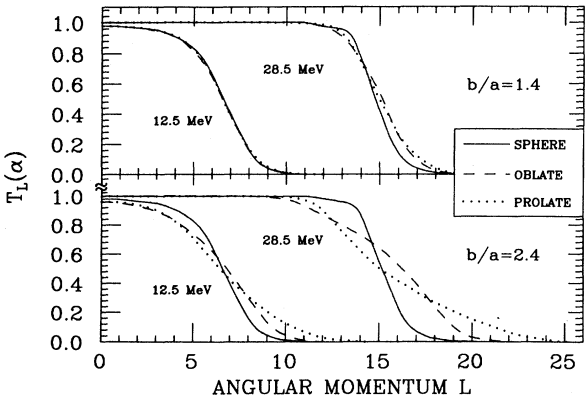

FIG. 5. α-particle transmission coefficients for the $^{63}Cu+\alpha$ reaction, as a function of angular momentum, are compared for spherical, oblate, and prolate deformations at center-of-mass energies of 12.5 and 28.5 MeV.

coefficients for deformed nuclei, due to the use of the Coulomb potential for spherical nuclei, is estimated to be small. This follows because the barrier radius as a function of θ is well outside the nuclear matter radius, defined by a Woods-Saxon potential as the radius, where the nuclear density has dropped to $\frac{1}{2}$ of the central density ρ_0, i.e., $\rho=\rho_0/2$. For symmetric prolate and oblate shapes, the Coulomb potential for deformed nuclei with *sharp* surfaces has been given by Swiatecki (quoted in Ref. 38). This potential for a prolate deformation of $b/a=2.4$ on the surface at a point ($x=b=1.793R$, $y=0$; the tip of the prolate spheroid) is 0.719 times the Coulomb potential on the surface of a sphere of radius R. Hence at the point ($x=1.793R$, $y=0$), the Coulomb potential for a deformed nucleus is 1.29 times the spherical nucleus Coulomb potential at this distance. As x increases, this difference in Coulomb energy decreases. In general, when the nuclear potential is included, the height of the barrier in the direction of the long axis is only slightly underestimated when the spherical nucleus charge distribution is used. At the other extreme for the point ($x=0$, $y=a=0.747R$) the barrier is slightly overestimated. Hence, the effective barrier height, obtained by weighting with the surface area, is rather insensitive to the type of Coulomb potential employed. In summary, the spherical nucleus charge distribution favors slightly, emission along the long axis relative to the short axis. In order to make realistic estimates of α-particle decay from deformed nuclei, it is essential to consider emission from all elements of the nuclear surface and not just emission along the long axis[29] of the nucleus where the barrier is the lowest. Hence, all α-particle transmission coefficients employed here in statistical-model calculations, are derived by weighting over the appropriate surface area. When this is done, the resulting α-particle transmission coefficients at moderate energies for oblate and prolate deformations with $b/a=1.4$ are very nearly identical to those for a sphere (see Fig. 3). Somewhat similar results are obtained even for very large deformations (see Fig. 4). However, as seen in Fig. 5 for $b/a=2.4$, angular momenta are possible well beyond the cutoff for spherical nuclei. Although the transmission coefficients for deformed nuclei calculated by the above method are approximate, due to fundamental and practical deficiencies in the calculational procedure, they should be sufficiently reliable to give a first-order estimate of the effect of nuclear deformation on particle spectra. In all calculations of transmission coefficients for deformed nuclei presented here, it is assumed for simplicity that the deformation is the same for all values of nuclear spin I, and that this deformation remains fixed throughout the deexcitation cascade. Such assumptions give an upper limit for the effects of deformation on the transmission coefficients.

III. MODEL CALCULATIONS

At the high excitation energies and spins of composite nuclei from heavy-ion-induced reactions, the evaporation spectra are very complex. Figure 6 illustrates the com-

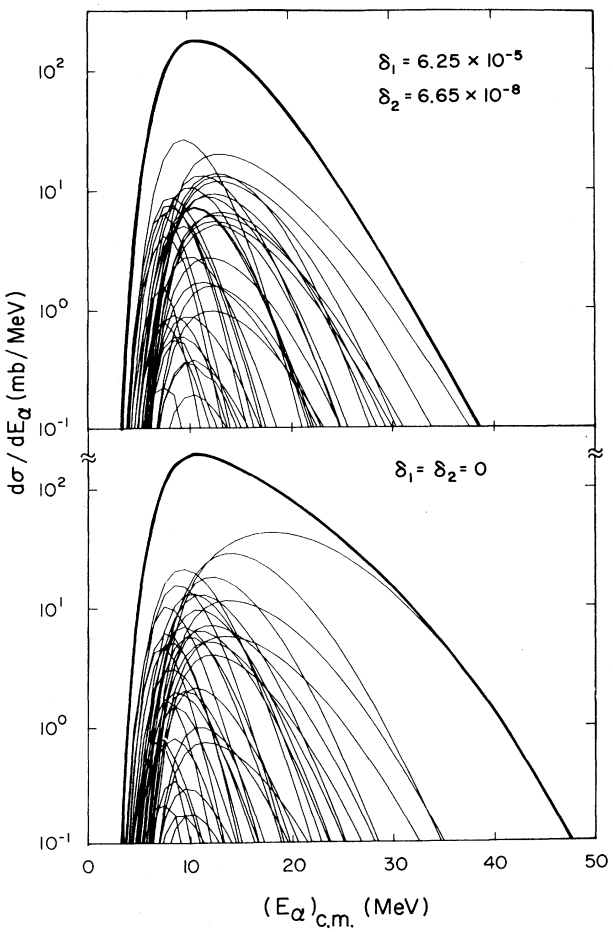

FIG. 6. Theoretical α-particle spectra calculated with a statistical model for the reaction $^{27}Al+^{40}Ar$ ($E_{lab}=190$ MeV). The thin solid lines are individual α spectra for each of the nuclei in the evaporation cascade (more than one spectrum results when an emitting nucleus is formed by multiple cascade paths). Each thick solid line is the total α spectrum produced by summing all the α spectra of the nuclei in the cascade. The bottom and top parts of the figure are for two different spin-dependent level densities [see Eq. (2)].

plexity hidden in the theoretical cumulative spectrum of α particles from the various stages of the cascade starting with the composite nucleus ^{67}Ga produced in the ^{27}Al+^{40}Ar ($E_{lab}=190$ MeV) reaction. The calculation assumes an initial excitation energy of 91 MeV and a spin distribution with a diffuse ($2\hbar$) edge located approximately at $I=46$. There are usually several cascade paths (see Fig. 7) on the (N,Z) plane that lead to any of the various α-emitting nuclides and thus contribute their respective individual α-particle spectra (thin curves in Fig. 6) to the cumulative spectrum (heavy curve in Fig. 6). The latter is the predicted theoretical spectrum to be compared to the inclusive experimental one.

The influence of the spin-dependent level density on the theoretical α-particle spectrum can be seen by comparing the top and bottom parts of Fig. 6. The curves in the top part of Fig. 6 are calculated with E_I [see Eq. (2)] values generated with $\delta_1=6.25\times10^{-5}$ and $\delta_2=6.65\times10^{-8}$, whereas the curves in the bottom part of Fig. 6 result for $\delta_1=\delta_2=0$. In each case, the maximum of the cumulative spectrum occurs at a significantly lower energy than the maximum of the spectrum for first chance α-particle emission (the most energetic individual spectrum). As a matter of fact, the position of the maximum in the cumulative theoretical spectrum can be seen in Fig. 6 to be rather insensitive to the particular change in the spin dependence of the level density introduced through E_I. The spin-dependent level density has its most profound influence on the shape of the high-energy tail of the cumulative spectrum.

A quantitative account of the complexity of the deexcitation cascade for ^{67}Ga is given in Fig. 7, where multiplicities of evaporated particles are given for the case, $\delta_1=6.25\times10^{-5}$ and $\delta_2=6.65\times10^{-8}$. The numbers on vertical, horizontal, and 45° lines in Fig. 7 are individual multiplicities of protons, neutrons, and α particles, re-

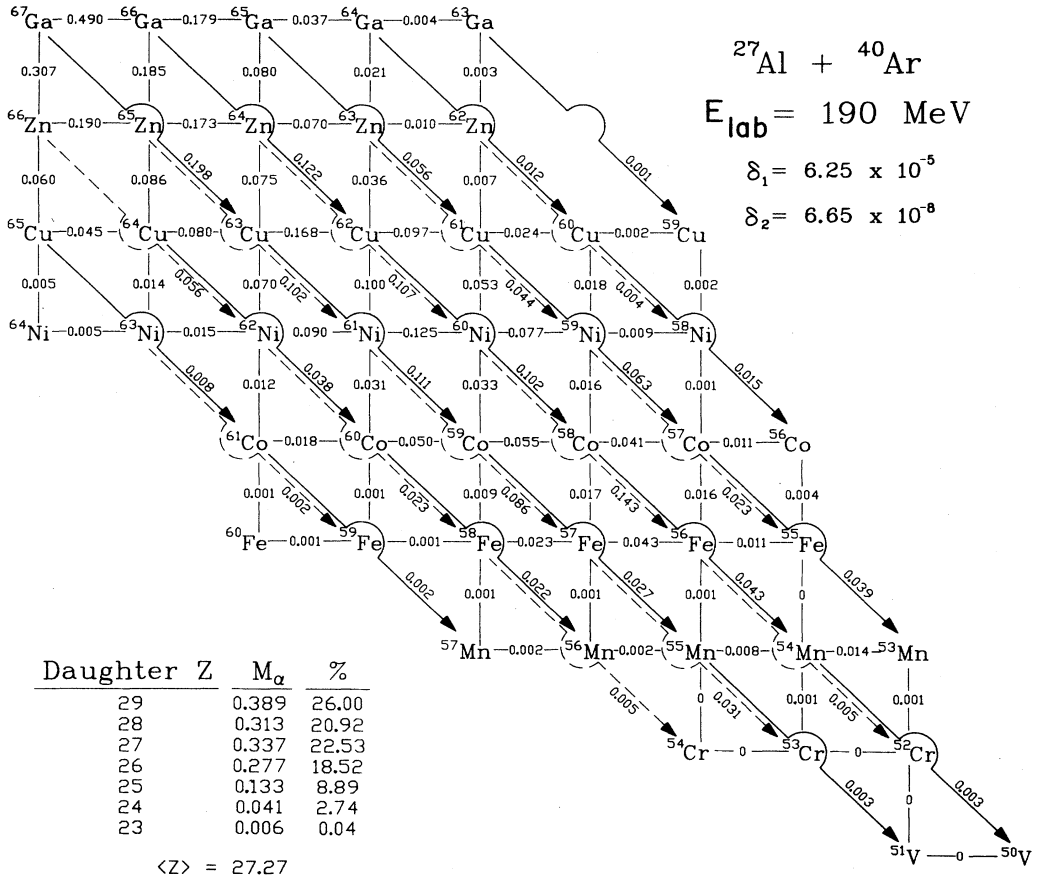

FIG. 7. Theoretical cascades of neutrons, protons, and α particles resulting from the reaction ^{27}Al+^{40}Ar ($E_{lab}=190$ MeV). The tabulated multiplicities of evaporated particles are based on a slightly modified version of the statistical model computer code CASCADE (Ref. 32). This figure illustrates the complexity of the deexcitation processes following the initial formation of the compound nucleus ^{67}Ga. The numbers on the vertical, horizontal, and 45° lines are individual multiplicities of protons, neutrons, and α particles, respectively. On the lower left part of the figure, the α-particle multiplicities associated with the Z values of seven different daughter nuclei are listed.

spectively. Of the 31 nuclides contributing to the total α-particle multiplicity, 22 nuclides contribute multiplicities equal to or greater than 0.010. The number of individual spectra shown in Fig. 6 even exceeds 31 because a few nuclei, e.g., ^{63}Cu, that can be formed by different paths, produce multiple spectra. When comparing experimental and theoretical spectra, it is imperative to realize that the cumulative spectra are a superposition of a large number of contributions from many nuclides in the complex cascade with different Z values, excitation energies and spins. It is understandable that simplified statistical-model codes such as GANES,[39] considering only single-chance emission from a nucleus at a single effective excitation energy and spin, are not able to fit such complex data by using standard statistical-model parameters.[25,27,28,30] Furthermore, in the simulation of experimental spectra with a single-chance emission code, the choice of the representative emitting nucleus is not clear. As can be seen in Fig. 7 (lower left), the total α-particle multiplicity has contributions from several elements, where on average, the emitting nucleus has a nearly 2 units smaller Z than the initial compound nucleus. Hence, the superposition of contributions from nuclei over a range in Z in the complex cascade leads to a peak in the cumulative spectrum that is significantly lower in energy than that of the first-chance α-emission spectrum.

As already illustrated in Fig. 6, the spin dependence of E_I has a pronounced effect on the cumulative α-particle spectra. In going from the $\delta_1=\delta_2=0$ case (Fig. 6, bottom) to the $\delta_1=6.25\times10^{-5}$, $\delta_2=6.65\times10^{-8}$ case (Fig. 6, top), the available phase space for low l-wave emission of neutrons and protons from the high-spin composite nuclear states is enhanced relative to the higher l-wave emission of α-particles from these states. As a result, the now strongly competing, neutron and proton emission suppresses the early-chance emission of alpha particles from the high-spin states. Direct confirmation of the role of the density of high-spin states on first-chance α-particle emission from ^{67}Ga is shown in Fig. 8, where the cross section for the two individual spins shown is normalized to the total compound nucleus cross section. For spin $\frac{91}{2}$, the first-chance α-particle spectrum for $\delta_1=\delta_2=0$ (heavy-dashed line at the bottom of Fig. 8) is very much harder and more intensive than the first-chance α-particle spectrum for $\delta_1=6.25\times10^{-5}$ and $\delta_2=6.65\times10^{-8}$ (light-dashed line at the bottom of Fig. 8). The enhanced-first chance neutron and proton emission for the latter case, and hence, the sizable reduction in the first-chance α-particle emission causes a marked change in the high-energy portion of the total α-particle spectrum (light and heavy solid lines at the bottom of Fig. 8). Depending on the form of the spin dependence of the level density of the high-spin states, as expressed by the values of δ_1 and δ_2, α-particle evaporation may be either enhanced or reduced relative to proton and neutron evaporation. This change in the first-chance α-particle emission probability has a profound effect on the intensity and slope of the high-energy portion of the α-particle spectrum, and the most probable energy in the first-chance α-particle spectrum for large spins is extremely sensitive to the spin dependence of the level density. However, the energy of the maximum of the cumulative spectrum is relatively insensitive to the choice of the values of the δ parameters as shown in Fig. 6. As seen in Fig. 8 (bottom, heavy- and light-dashed lines) this most probable energy decreases for $I=\frac{91}{2}$ by over 7 MeV when the values of the parameters δ_1 and δ_2 are increased from $\delta_1=\delta_2=0$ to $\delta_1=6.25\times10^{-5}$ and $\delta_2=6.65\times10^{-8}$. With these latter parameters values, the first-chance most probable energy for $I=\frac{91}{2}$ is reduced drastically to approximately the same most probable energy as the corresponding peak for $I=\frac{51}{2}$, which exhibits only little sensitivity to the values of δ_1 and δ_2. This is true also for the energy of the maximum of the cumulative spectrum which is relatively independent of the choice of parameter values, as shown in Fig. 6. Figure 8 demonstrates this insensitivity of the most probable α-particle energy of the cumulative spectrum, for individual spins as large as $\frac{91}{2}$. This result is due to the complexity of the cascade and the importance of contributions from later stages in the

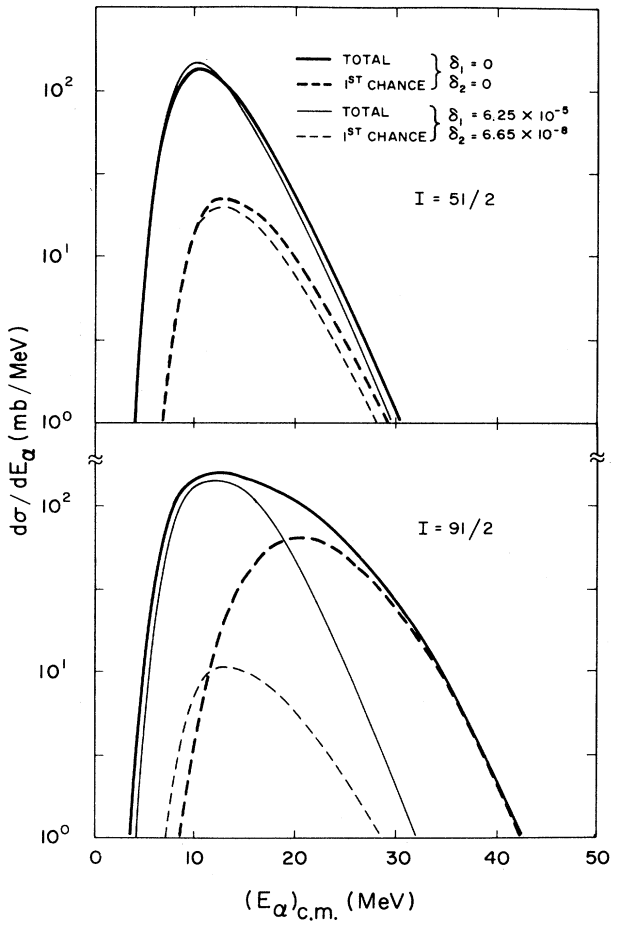

FIG. 8. Similar to Fig. 6, except for selected spins of $\frac{51}{2}$ and $\frac{91}{2}$ (normalized to the total compound nucleus cross section). This figure illustrates the suppression of first-chance α emission for very large spins when realistic values of δ_1 and δ_2 are introduced.

cascade in the establishment of the most probable α energy.

In Fig. 9, the theoretical α-particle spectra are calculated with α-particle transmission coefficients for prolate ($b/a=1.4$), oblate ($b/a=1.4$), and spherical ($b/a=1.0$) nuclei. Again, these calculations are for the $^{27}Al+^{40}Ar$ ($E_{lab}=190$ MeV) reaction, and the same spin-dependent level density is used in all the three cases, in order to study the effect of the different sets of α-particle transmission coefficients on the spectra. Neither the individual spectra nor the cumulative spectrum are altered significantly when α-particle transmission coefficients for moderately ($b/a=1.4$) deformed nuclei are used in the theoretical calculations. For the sake of calibration, an oblate deformation of $b/a=1.4$ is that predicted by the RLDM for ^{63}Cu with a spin of approximately 40. Hence, for the spin distribution (and corresponding RLDM deformations) populated in the above reaction, the use of spherical and deformed nucleus transmission coefficients leads to very similar α-particle evaporation spectra. This is consistent with expectations since the effective barriers for prolate and oblate nuclei with $b/a=1.4$ are very nearly equal to those for spherical nuclei (see Fig. 3). However, if the deformation is increased to $b/a=2.4$, the theoretical cumulative α-particle spectra calculated with α-particle transmission coefficients for prolate and oblate nuclei have a greater intensity of high-energy α particles than for the spherical nucleus case, as illustrated in Fig. 10. The three cumulative spectra in Fig. 10 are calculated for the $^{27}Al+^{40}Ar$ ($E_{lab}=190$ MeV) reaction with $\delta_1=3.32\times10^{-5}$ and $\delta_2=2.95\times10^{-8}$. It is significant to observe, however, that despite this change in the high-energy tails of the spectra, the most probable α-particle energy of each cumulative spectrum is nearly the same. This characteristic feature of cumulative spectra, a property that results from the superposition of a large number of spectra associated with a complex cascade, has been discussed previously.

The spin dependence of the level density, effected by

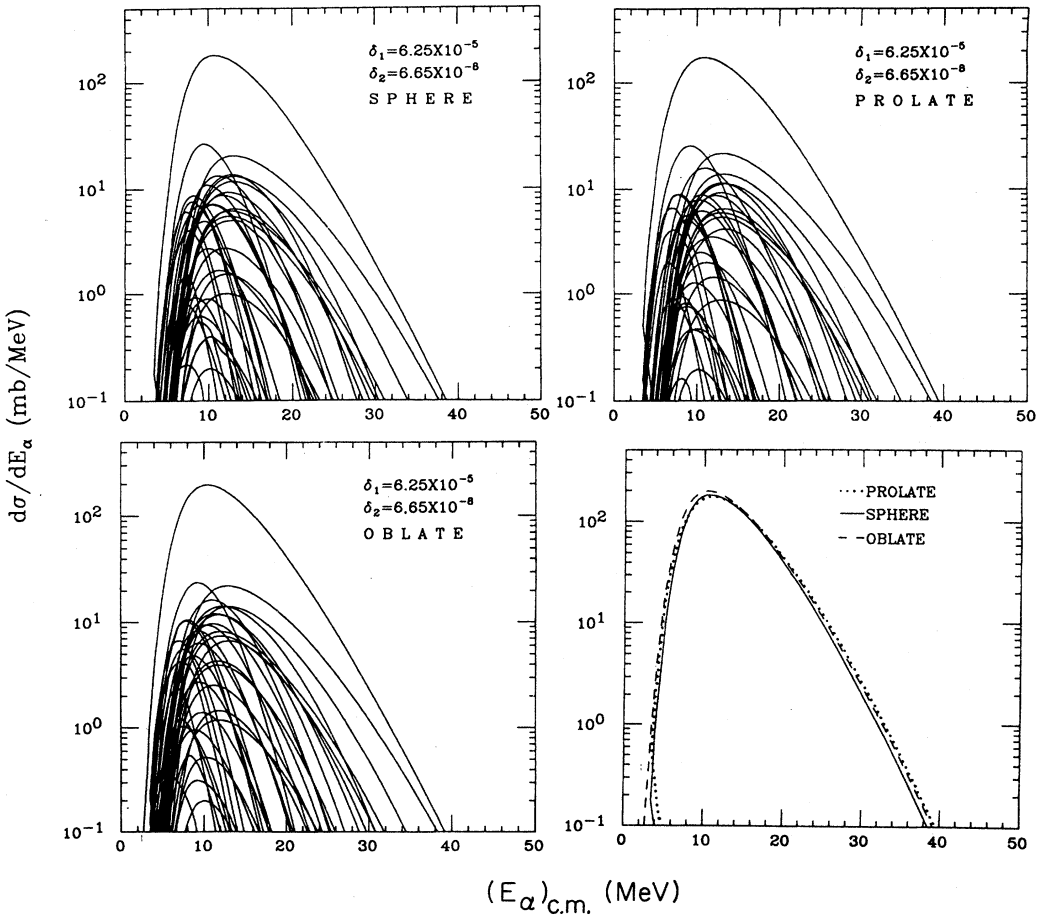

FIG. 9. Comparison of theoretical α-particle spectra (see Fig. 6) for the reaction $^{27}Al+^{40}Ar$ ($E_{lab}=190$ MeV) when α-particle transmission coefficients (see Figs. 3 and 5) are those of nuclei with spherical, prolate ($b/a=1.4$), and oblate ($b/a=1.4$) shapes (see Fig. 1). The lower right-hand-side display compares the total α-particle spectra for the three different nuclear shapes with the same spin-dependent level density (i.e., the same values of δ_1 and δ_2) illustrating the insensitivity of the results on the α-particle transmission coefficients for prolate and oblate transformations with $b/a=1.4$.

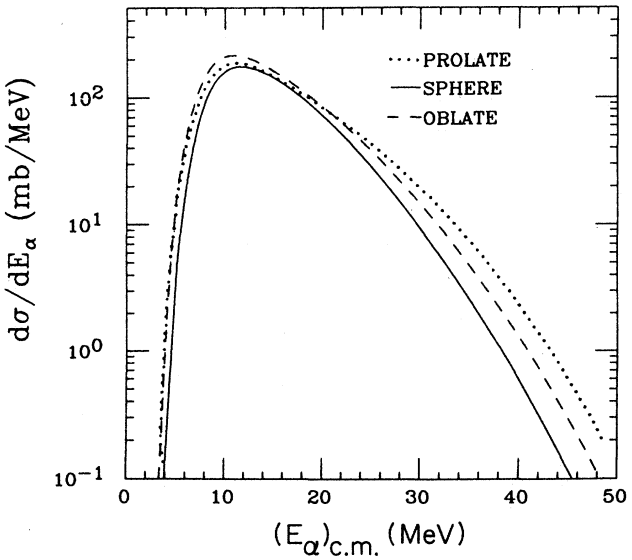

FIG. 10. Comparison of theoretical total α-particle spectra for the reaction ^{27}Al+^{40}Ar (E_{lab}=190 MeV) when the α-particle transmission coefficients (see Figs. 4 and 5) of nuclei in each cascade correspond to spherical, prolate (b/a=2.4), and oblate (b/a=2.4) shapes (see Fig. 1). The same spin-dependent level density is used for each calculation ($\delta_1=3.32\times10^{-5}$ and $\delta_2=2.95\times10^{-8}$), illustrating the effects of deformation on the total α-particle spectra due to the different α-particle transmission coefficients.

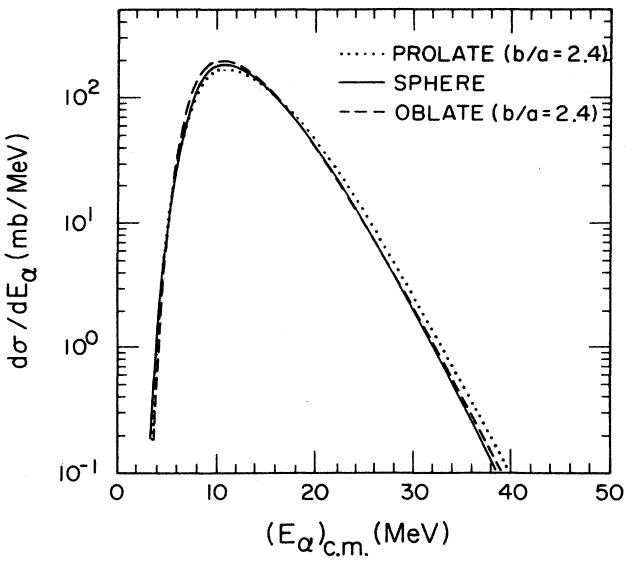

FIG. 11. The same transmission coefficients are used as Fig. 10, except more realistic spin-dependent level densities are employed; spherical, $\delta_1=6.25\times10^{-5}$, $\delta_2=6.65\times10^{-8}$; prolate, $\delta_1=1.41\times10^{-4}$, $\delta_2=1.47\times10^{-7}$; oblate, $\delta_1=1.22\times10^{-4}$, $\delta_2=1.33\times10^{-7}$. It should be noted that for the spherical nucleus calculation, the transmission coefficients are calculated for a spherical nucleus, however, the level density is that appropriate for a deformed nucleus with b/a of approximately 1.4 (see Fig. 9).

variations in E_I vs I via the δ_1 and δ_2 values, produces a noticeable change in the slope of the high-energy tail of the spectrum, but not in the peak position as described in the previous paragraph. Increasing δ_1 and δ_2 (reducing the values of E_I) enhances the available phase space for low l-wave emission of neutrons and protons from high-spin compound nuclear states relative to the higher l-wave emission of α particles from these states. As a result, the more strongly competing neutron and proton emission suppresses the early-chance emission of α particles from the high-spin states. It is the first-chance α-particle emission from the high-spin states in ^{67}Ga that is responsible for the high-energy part of the cumulative spectrum (see, e.g., Fig. 6 and the bottom part of Fig. 8). The suppression of first-chance α-particle emission leads to a substantial softening of the high-energy part of the cumulative spectrum. The important lesson to be learned from these results is that nucleon emission can compete effectively with heavier-particle emission in the statistical decay of high-spin states, the competition depending on the spin-dependent level density. This result is often not appreciated.

The greater intensity of high-energy events in the theoretical cumulative α-particle spectra calculated with

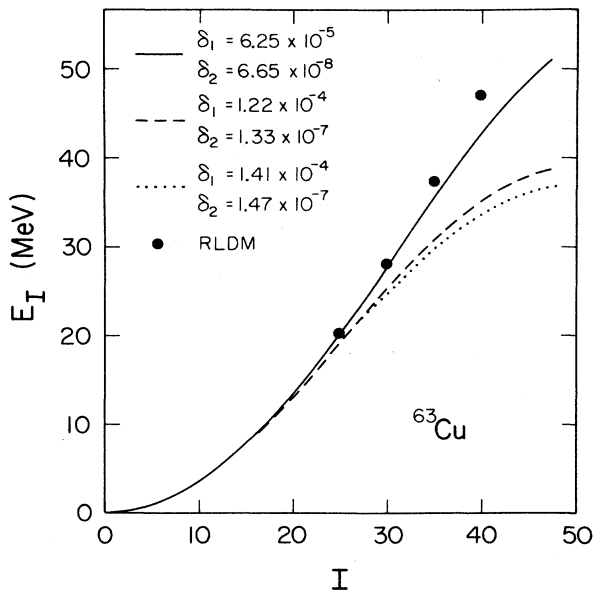

FIG. 12. Values of E_I for the nucleus ^{63}Cu as a function of I for different sets of δ values [see Eq. (2)]. The solid line represents E_I values used in the analysis of the experimental (Ref. 25) α-particle spectra for the ^{27}Al+^{40}Ar (E_{lab}=190 MeV) reaction (see Fig. 13). The E_I values given by the solid, dashed, and dotted lines were used to calculate the theoretical spectra displayed Fig. 11. The solid points represent the sum of the collective rotational and deformation energies given by the RLDM (Ref. 31). Since CASCADE (Ref. 32) uses a variable and somewhat larger radius parameter than does the RLDM, the RLDM energies plotted are relative to the energy of a rotating rigid sphere (see Fig. 12 of Ref. 31) with the radius parameter used in CASCADE.

α-particle transmission coefficients for nuclei with large deformations ($b/a=2.4$) can be readily suppressed by reducing the spin dependence of the level density of the high-spin states. This is illustrated in Fig. 11, differing from Fig. 10 only by the δ values. The corresponding E_I values, used to calculate the theoretical cumulative spectra in Fig. 11, are illustrated in Fig. 12 for the single nucleus ^{63}Cu in the cascade. The important conclusion to be drawn from these figures is that there are opposing effects of deformation on the theoretical cumulative spectrum, introduced by the transmission coefficients on the one hand, and on the other hand, by the spin-dependent level density $\rho(E,I)$ that depends directly in E_I in the present formalism. As can be seen in Fig. 11, the cumulative spectra for the three cases are essentially the same, illustrating the insensitivity of such spectra to the deformation expected for composite nuclei produced with large excitation energies and high spins.

IV. COMPARISON OF EXPERIMENTAL AND THEORETICAL CUMULATIVE SPECTRA

In Fig. 13, statistical model calculations of cumulative spectra are compared to experimental α-particle spectra[25] for the reaction ^{27}Al+^{40}Ar ($E_{\rm lab}=190$ MeV), measured at four laboratory angles. As already described in Sec. II, appropriate absorption channel values of transmission coefficients were employed in the calculations for all particle evaporation channels. Fission was also taken into account. Input parameter values of $\delta_1=6.25\times10^{-5}$ and $\delta_2=6.65\times10^{-8}$ were chosen to parametrize E_I [see Eq. (2)] which defines the spin-dependent level density [see Eq. (1)]. Since CASCADE does not calculate angular distributions, the experimental angular distribution[25] was adopted in the calculations. In Fig. 14, the experimental angular distribution of α particles for the ^{27}Al+^{40}Ar reaction at $E_{\rm lab}=190$ MeV is compared to that calculated with the statistical-model code PACE,[40] which predicts angular distributions but treats transmission coefficients in a more approximate fashion. The solid circles represent experimental data[25] at average center-of-mass angles, and the solid line was calculated directly from the laboratory energy spectra.

As can be seen from Fig. 13, the agreement between experiment and statistical-model calculations is excellent, insofar as the shapes of the spectra are concerned. Equally impressive agreement is achieved with α-particle transmission coefficients for prolate ($b/a=1.4$), oblate ($b/a=1.4$), and spherical nuclei (see Fig. 9). In addition, there is also very good agreement between theory and experiment with respect to α-particle multiplicity, as evidenced by the excellent fits to the double differential cross sections at the four angles.

If one interprets the quantity E_I in Eq. (2) in a very limited way, i.e., in terms of the sum of collective rotational and deformation energies, it can be compared to the predictions of the rotating liquid drop model.[31] Such a comparison shows that at high spins, the values of E_I shown in Fig. 12 (solid line) and needed to reproduce the data in Fig. 13 are somewhat smaller than predicted by the RLDM. For example, the discrepancy is of the order of 2% at $I=30$ and 10% at $I=40$. It must be emphasized, however, as discussed in Sec. II, that the quantity E_I has a much more complex interpretation.

Analyses similar to those described above were performed also for the ^{64}Ni+^{19}F and ^{27}Al+^{32}S compound nucleus reactions. The experimental α-particle spectra measured at four angles for the ^{64}Ni+^{19}F ($E_{\rm lab}=120$ MeV) reaction[28] are plotted in Fig. 15 along with the respective cumulative spectra calculated with the statistical-model code CASCADE. The initial excitation energy and maximum angular momentum are 103 MeV and 47$\hbar$, respectively. As can be seen in Fig. 15, the agreement between experiment and statistical theory is very good both in terms of the spectral shapes and the absolute differential cross sections. The values of E_I ($\delta_1=4.5\times10^{-5}$ and $\delta_2=3.5\times10^{-8}$) as a function of I used in the calculations are plotted in Fig. 16. Also

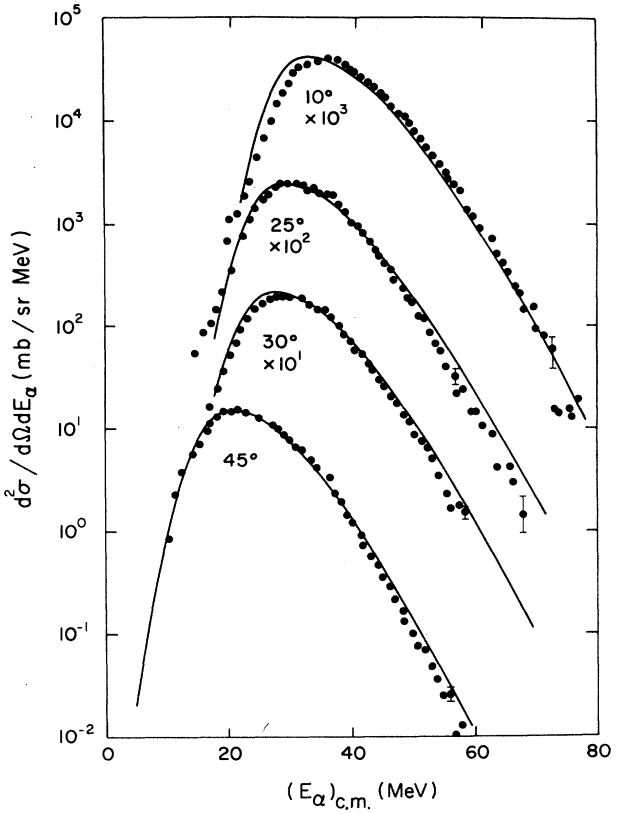

FIG. 13. Comparisons of statistical-model and experimental (Ref. 25) α-particle spectra for the reaction ^{27}Al+^{40}Ar ($E_{\rm lab}=190$ MeV). The statistical-model α-particle spectra are calculated with α-particle transmission coefficients for spherical nuclei and $\delta_1=6.25\times10^{-5}$ and $\delta_2=6.65\times10^{-8}$. Essentially identical α-particle spectra are obtained with α-particle transmission coefficients for prolate ($b/a=1.4$) and oblate ($b/a=1.4$) nuclei (see Fig. 9). The fits remain almost equally good with α-particle transmission coefficients for highly deformed ($b/a=2.4$) nuclei if realistic values of δ_1 and δ_2 are employed (see text and Fig. 11).

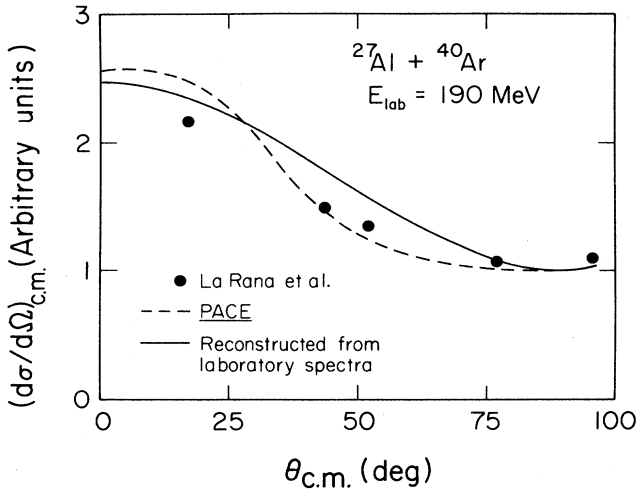

FIG. 14. Angular distribution of α particles for the ^{27}Al+^{40}Ar reaction at a laboratory bombarding energy of 190 MeV. The circles were reported by Ref. 25 and represent data at $\langle\Theta_{c.m.}\rangle$. The solid line was calculated directly from the laboratory spectra reported by Ref. 25. The dashed line was calculated with the code PACE (Ref. 40).

shown in this figure, for several spin values, are the sums of the collective rotational and deformation energies predicted by the RLDM. For the spin range excited in this reaction, the maximum difference between the E_I values and the sum of RLDM rotational and deformation energies is of the order of 10%. Based on the present statistical model fits to the α-particle spectra from the ^{64}Ni+^{19}F reaction, no evidence is obtained from this case either to support the unusually large deformations of $b/a=2.2$ deduced[28] from calculations with the one-step decay code GANES.[39]

The experimental α-particle spectra reported for the ^{27}Al+^{32}S reaction,[26,29] at six laboratory bombarding energies, ranging from 100 to 150 MeV, are shown in Fig. 17 along with the respective cumulative spectra calculated with the statistical-model code CASCADE. The initial excitation energy in the compound nucleus ranges from 59 to 81 MeV, while the maximum angular momentum varies from 27 to 42$\hbar$. The largest values of the initial energy and angular momentum of the compound nucleus excited in this reaction are somewhat smaller than the values of the corresponding quantities for the two reactions discussed previously. Good agreement between experiment and theory is obtained for the shapes of the cumulative spectra with values of E_I derived from Eq. (2) with $\delta_1=1.25\times10^{-4}$ and $\delta_2=1.17\times10^{-7}$. In Fig. 18 the values of E_I derived with those parameters are plotted as a solid line. At the higher-spin values, the values of E_I used in the calculations are somewhat smaller than the sum of the collective rotational and deformation energy predicted by the RLDM (see solid circles in Fig. 18). Since the double-differential cross sections of α particles are reported[26,29] in relative units, no comparison can be made between the experimental and theoretical α-particle multiplicity as was done for the two reactions studied previously.

Previous statistical-model fits[26,29] to the α-particle spectra from the ^{27}Al+^{32}S reaction using a similar computer code to follow the complex decay cascade differ in two important aspects from the present calculations. First, the optical-model potential transmission coefficients were calculated for a spherical nucleus with a radius enlarged by factors increasing with increasing bombarding energy (1.25 for $E_{lab}=150$ MeV). The motivation for this was to account for the deformation in the calculation of the transmission coefficients. As discussed above, with deformations predicted by the RLDM for the highest spins excited in this reaction, the effective barrier calculated by weighting over the surface area is essentially unchanged from that for the spherical nucleus (see Fig. 3). Furthermore, the increase in radius is somewhat equivalent to the assumption that all charged parti-

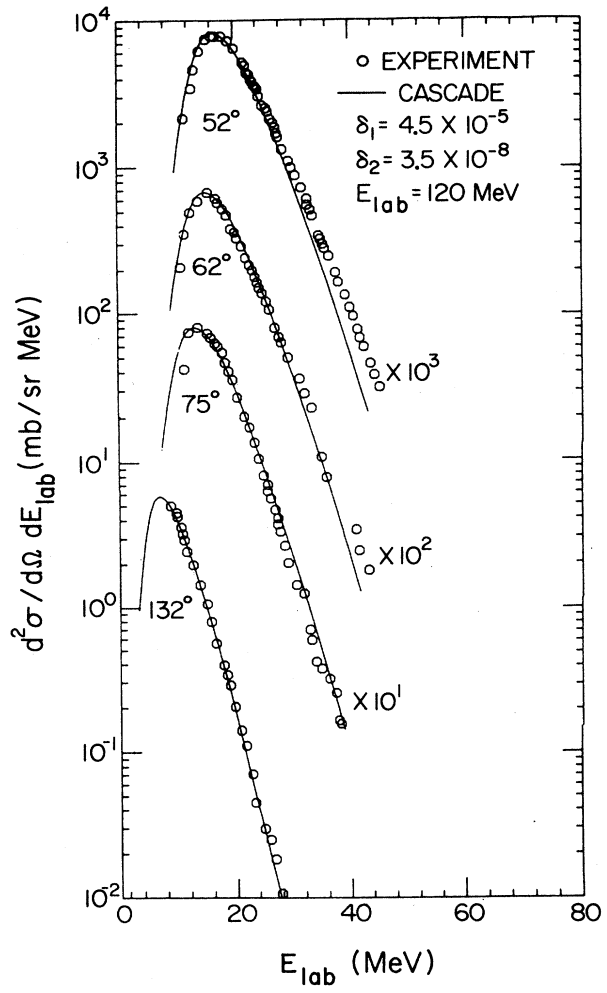

FIG. 15. Comparisons of statistical-model and experimental (Ref. 28) α-particle spectra for the reaction ^{64}Ni+^{19}F ($E_{lab}=120$ MeV).

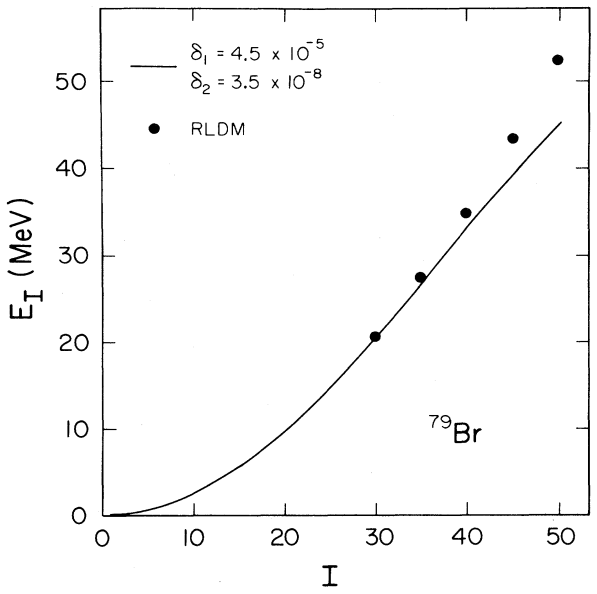

FIG. 16. Values of E_I for the nucleus ^{79}Br as a function of I for $\delta_1 = 4.5 \times 10^{-5}$ and $\delta_2 = 3.5 \times 10^{-8}$. The solid circles represent the sum of the collective rotational and deformation energies given by the RLDM (Ref. 31). See caption of Fig. 12.

cles are emitted from the tips of a prolate nucleus, excluding most of the surface area. One of the results of the larger radii is more yield of high-energy α particles, than is compatible with experiment. In order to reduce the theoretical intensity of high-energy α particles, it is necessary to increase the level density of high-spin states. This is done in the calculations of Viesti *et al.*[29] by lowering the so-called effective yrast line. As shown in Fig. 18, the values of E_I used by Viesti *et al.*[29] (dashed line) are substantially smaller than the values used in the present calculation (solid line). These opposing effects of deformation on transmission coefficients and the spin-dependent level density have been discussed previously (see Figs. 10 and 11). Hence, if larger optical-model radii are used in the calculation, it is expected that one needs to lower the E_I values in order to reduce the intensity of high-energy α particles.

In each of the above cases, a statistical-model calculation using the code CASCADE reproduces the position of the maximum of the cumulative α-particle evaporation spectrum when the evaporation barrier of each nuclide in the cascade is assumed equal to its respective absorption channel barrier, i.e., no reduction in the respective barriers are required in the complex statistical-model calculations reported here. This conclusion is independent of the δ values used in the calculation, as illustrated in Fig. 6. Hence, the reported[25,27,28] unusually large nuclear deformations, deduced with the single-step evaporation code GANES,[39] is attributed to the simplifying approximations used in this latter code.

V. SUMMARY

The statistical model offers a conceptually simple, however, sound framework for interpreting various sets of experimental information on nuclear phenomena, and among them, on particle (evaporation) spectra from spinning excited nuclei. The underlying physical processes are, however, highly complex, not fully understood, and seldom allow for an accurate numerical representation. Therefore, in any practical implementation of this model, there are a number of assumptions and approximations that need to be made in order to derive numerical predictions, for any particular set of experimental data, from the simple original concepts. As a result, in the mathematical formulations of the model, simple conceptual physical quantities, such as, e.g., yrast energy, barrier height, level density parameter a, nuclear deformation, etc, are replaced by their effective counterparts, namely the effective barrier, effective a, effective deformation, and so on. The fact that such substitutions have

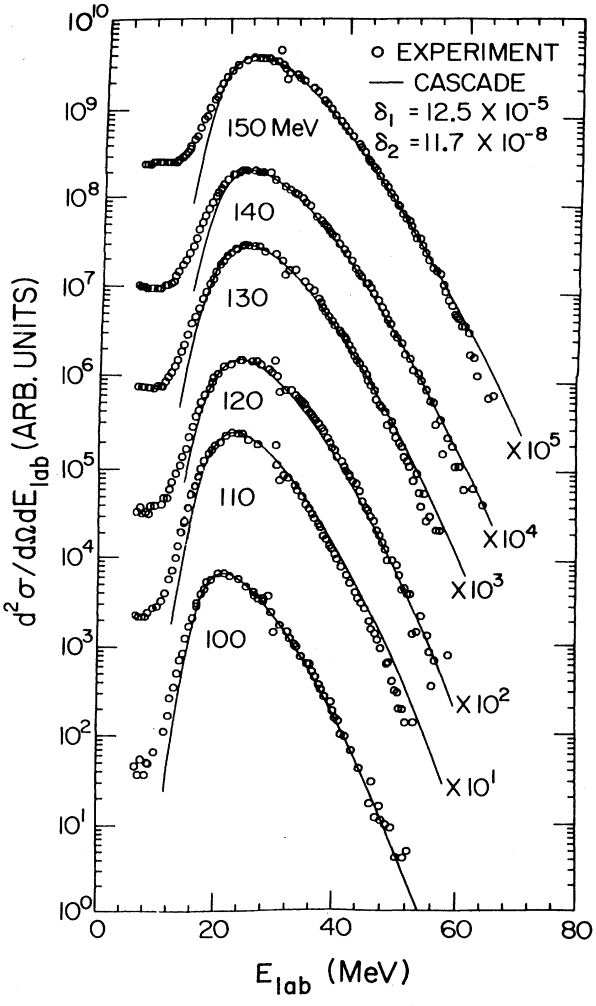

FIG. 17. Comparisons of statistical-model and experimental (Refs. 26 and 29) α-particle spectra for the reaction ^{27}Al+^{32}S at six laboratory bombarding energies ranging from 100 to 150 MeV. The experimental spectra, measured at $\Theta_{lab} = 30°$, have a sizable low-energy background. Subtraction of this background greatly improves the agreement between theory and experiment at small α energies.

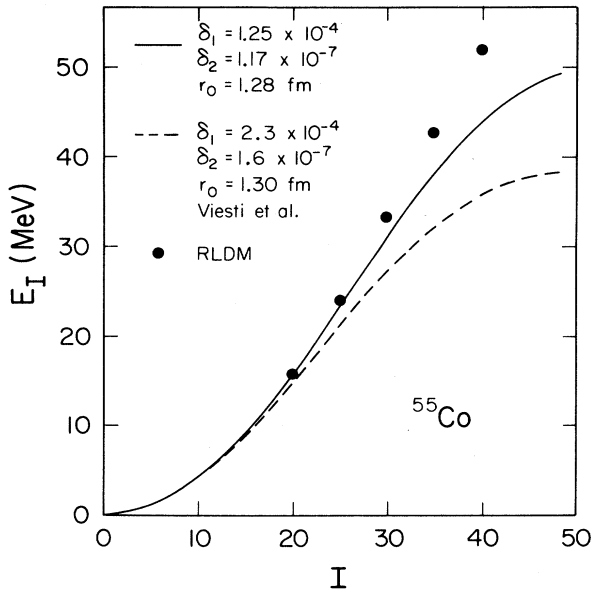

FIG. 18. Values of E_I for the nucleus ^{55}Co as a function of I for different sets of δ values [see Eq. (2)]. The solid line represents E_I values used in the present analysis of experimental data (Refs. 26 and 29) for the ^{27}Al+^{32}S reaction at laboratory energies ranging from 100 to 150 MeV (see Fig. 17). The dashed line was used in the analysis of the same data in Ref. 29. The solid circles represent the sum of the collective rotational and deformation energies given by the RLDM (Ref. 31). See caption of Fig. 12.

been implicitly made, has to be kept in mind when attempting to extract information on physical properties of nuclear systems based on statistical-model analysis of experimental data.

The present study has revealed, through various model calculations of the α-particle evaporation spectra, the effects of different assumptions and approximations on the values of the above effective quantities, most notably, on the effective nuclear deformation. This effective deformation appears both in simplified and in complete statistical decay cascade approaches.

The simplified approaches that have been probed, include a single-step effective cascade approach[25,27,28,30,39] as well as a very approximate approach based on analytical equations[19,20,23,41] for the α-particle energy spectra. It is shown, that in the case of high-spin, hot compound nuclei these approaches lead systematically to values of the effective barrier heights that are lower than those believed to reflect the physical barriers of colder, lower-spin systems, and consequently, they lead to the unusually large effective deformations. In view of the availability of complete statistical decay cascade codes such as CASCADE (Ref. 32) and PACE,[40] it appears then advisable not to pursue such approaches, at least as far as studying the deformation of spinning nuclei is concerned.

In complete statistical cascade calculations, the effective nuclear deformation appears as a common feature in the two distinct types of assumptions made, one concerning the available phase space (level density) and the other concerning the access to this space (transmission coefficients). Uncertainties in the choice of implementing each of these fundamental constituents of the statistical model, affect directly the deduced values of effective quantities, but the accepted choices can be justified only with a varying and often limited degree of confidence.

As far as the nuclear level-density calculations are concerned, the effective deformation enters Eqs. (1) and (2) through evaluation of the collective or macroscopic (deformation and rotational) portion of the nuclear excitation energy which does not contribute to the thermal energy. There are, however, many phenomena that are not included explicitly in the derivation of Eqs. (1) and (2), which affect the effective collective energy, and thus the effective deformation. So, e.g., the level-density parameter a is essentially unknown at high-spins and high excitation energies. Its value is affected by the deformation- and rotation-induced rearrangement of the single-particle level scheme on the one hand, and by the macroscopic effect of the altered nuclear surface area on the other. The latter effect is small at moderate deformations that are compatible with the RLDM, but becomes quite significant for higher deformations (see Fig. 19). It leads to an increase of a with increasing deformations[42] and, by virtue of the role of this parameter in the Fermi gas model, affects the temperature of the system. Thus, when not accounted for explicitly, it affects the effectie collective energy which, in turn, is reflected in the effective deformation. Apart from the fact that the link between the nuclear deformation and the macroscopic energy provided by the RLDM has its own uncertainties, the level density may be additionally enhanced (collective enhancement) as suggested in Ref. 43. In the present study, effects similar to the above are implicitly included in the values of the δ parameters. It is shown that the resulting effective deformations for the systems studied are compatible with the predictions of the RLDM for the nuclear deformation.

As far as the uncertainty introduced by the deformed

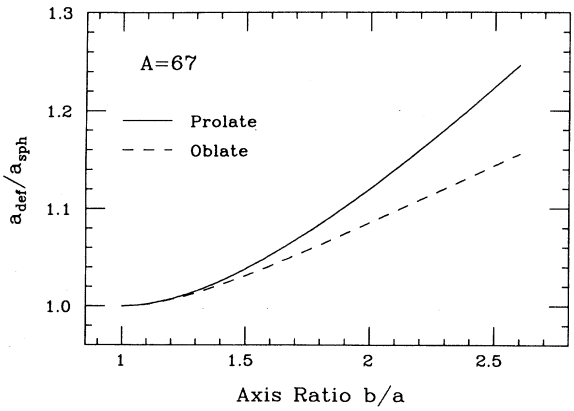

FIG. 19. The ratio of the level-density parameter of a deformed nucleus to that of a spherical nucleus as a function of b/a (see Ref. 42) for a nucleus with equally spaced single-particle levels.

nucleus transmission coefficients is concerned, it is shown that the effective barrier heights are fairly insensitive to the nuclear deformation when an averaging over the whole surface area of the nucleus is carried out. Such an averaging procedure, relying partially on classical and partially on quantum-mechanical approaches (optical model) has its own uncertainties, but appears superior to a simple increase of the radius parameter[29] in the optical-model calculations. The latter approach is shown to enhance the intensity of the high-energy α particles in the spectrum. Such an enhancement is then offset in the model calculations by an appropriate reduction of the (effective) collective energy which leads to an unusually large effective deformation.

In summary, it is shown that when no unnecessary approximations and simplifications are made in calculating the α-particle evaporation spectra from spinning hot nuclei, within the framework of the statistical decay model, the effective quantities and, in particular, the effective deformation deduced based on experimental data, are compatible with established systematics for their true physical counterparts. It is shown that previous claims of unusually large nuclear deformations at high-spin values result from the oversimplifications employed in the implementation of the statistical model.

This work was supported by the U.S. Department of Energy under Grant No. DE-FG02-88ER40414.

[1]I. M. Govil, J. R. Huizenga, W. U. Schröder, and J. Tōke, Phys. Lett. B **197**, 515 (1987).
[2]L. Wolfenstein, Phys. Rev. **82**, 690 (1951).
[3]J. M. Blatt and V. F. Weisskopf, *Theoretical Physics* (Wiley, New York, 1952).
[4]W. Hauser and H. Feshbach, Phys. Rev. **87**, 366 (1952).
[5]T. Ericson and V. Strutinsky, Nucl. Phys. **8**, 284 (1958); **9**, 689 (1959).
[6]A. M. Lane and R. G. Thomas, Rev. Mod. Phys. **30**, 257 (1958).
[7]A. C. Douglas and N. MacDonald, Nucl. Phys. **13**, 382 (1959).
[8]T. Ericson, Adv. Phys. **9**, 425 (1960).
[9]E. Vogt, *Advances in Nuclear Physics,* edited by M. Baranger and E. Vogt (Plenum, New York, 1968), Vol. I, p. 261.
[10]R. G. Stokstad, in *Treatise on Heavy-Ion Science,* edited by D. A. Bromley (Plenum, New York, 1985), Vol. 3, p. 83.
[11]R. W. West, Phys. Rev. **141**, 1033 (1966).
[12]M. J. Fluss *et al.*, Phys. Rev. **187**, 1449 (1969).
[13]C. C. Lu, J. R. Huizenga, C. J. Stephan, and A. J. Gorski, Nucl. Phys. **A164**, 225 (1971).
[14]L. C. Vaz, C. C. Lu, and J. R. Huizenga, Phys. Rev. C **5**, 463 (1972).
[15]C. C. Lu, L. C. Vaz, and J. R. Huizenga, Nucl. Phys. **A190**, 229 (1972).
[16]C. C. Lu, L. C. Vaz, and J. R. Huizenga, Nucl. Phys. **A197**, 321 (1972).
[17]J. R. Huizenga and L. G. Moretto, Annu. Rev. Nucl. Sci. **22**, 427 (1972).
[18]J. Wiley, J. C. Pacer, C. R. Lux, and N. T. Porile, Nucl. Phys. **A212**, 1 (1973).
[19]M. F. Rivet *et al.*, Phys. Rev. C **25**, 2430 (1982).
[20]J. M. Alexander, D. Guerreau, and L. C. Vaz, Z. Phys. A **305**, 313 (1982).
[21]L. C. Vaz *et al.*, Z. Phys. A **315**, 169 (1984).
[22]R. K. Choudhury *et al.*, Phys. Lett. **143B**, 74 (1984).
[23]G. Nebbia *et al.*, Phys. Lett. B **176**, 20 (1986).
[24]Z. Majka *et al.*, Phys. Rev. C **35**, 2125 (1987).
[25]G. LaRana *et al.*, Phys. Rev. C **35**, 373 (1987).
[26]B. Fornal *et al.*, Phys. Rev. C **37**, 2624 (1988).
[27]G. LaRana *et al.*, Phys. Rev. C **37**, 1920 (1988).
[28]G. LaRana *et al.*, in *Third International Conference on Nucleus-Nucleus Collisions, Saint-Malo, France, 1988,* edited by C. Esteve, C. Gregoire, D. Guerreau, and B. Tamain (Centre de Publications de L'Universite de Caen, Caen, 1988), p. 81.
[29]G. Viesti *et al.*, Phys. Rev. C **38**, 2640 (1988).
[30]G. F. Peaslee *et al.*, Phys. Rev. C **39**, 488 (1989).
[31]S. Cohen, F. Plasil, and W. Swiatecki, Ann. Phys. (N.Y.) **82**, 557 (1974).
[32]F. Puhlhofer, Nucl. Phys. **A280**, 267 (1977).
[33]D. W. Lang, Nucl. Phys. **77**, 545 (1966).
[34]F. C. Williams, Jr., G. Chan, and J. R. Huizenga, Nucl. Phys. **A187**, 225 (1972).
[35]E. Hodgson, Annu. Rev. Nucl. Sci. **17**, 1 (1967).
[36]F. G. Perey, Phys. Rev. **131**, 745 (1963).
[37]J. R. Huizenga and G. Igo, Nucl. Phys. **29**, 462 (1961).
[38]M. Blann, Phys. Rev. C **21**, 1770 (1980); the denominator in Eq. (11) should read 2ϵ instead of 3ϵ.
[39]N. N. Ajitanand *et al.*, Nucl. Instrum. Methods **A243**, 111 (1986).
[40]A. Gavron, Phys. Rev. **20**, 230 (1980).
[41]M. Gonin *et al.*, Phys. Lett. B **217**, 406 (1989).
[42]J. Tōke and W. J. Swiatecki, Nucl. Phys. **A372**, 141 (1981).
[43]S. Bjørnholm, A. Bohr, and B. R. Mottelson, *Proceedings of the Third International Symposium on the Physics and Chemistry of Fission, Rochester, 1973* (IAEA, Vienna, 1974), Vol. 1, p. 367.